JOURNAL OF MATERIALS SCIENCE 11 (1976) 1979–1988

Assessment of the fracture toughness of cast steels

Part 1 *Low alloy steels*

J. T. BARNBY, I. S. AL-DAIMALANI
Department of Metallurgy and Materials, University of Aston, Birmingham, UK

Estimates of the fracture toughness in terms of the critical stress intensity factors K_C and K_{IC} are made for a 1Cr steel, a $\frac{1}{2}$Cr–$\frac{1}{2}$Mo–$\frac{1}{4}$V steel, a $1\frac{1}{2}$Mn–Ni–Cr–Mo steel and a $1\frac{1}{2}$Ni–Cr–Mo steel all in cast form. The methods used are linear elastic fracture mechanics, *J*-integral and crack opening displacement methods. The last two methods are applied in combination with an electrical potential method to detect the initiation of fracture.

1. Introduction

Cast steels are a special class of engineering materials controlled by their own special standards [1]. Only where exhaustive non-destructive testing has shown them to be defect free are they allowed to bear the same working stresses as wrought steels, as, for instance, in pressure containment situations [2]. Defect control in cast steels bears little relation to the defect tolerance of the particular steel based on fracture toughness since defects are classed as deleterious more or less on the basis of whether they are detectable by radiographic methods [3]. Although these methods are probably adequate and based on practical experience for the highest strength castings, they bear little relevance to the real defect tolerance of the more commonly used steels. Often the integrity of a casting is reduced by cutting out small casting defects and repair welding [4].

Since little information on K_C or K_{IC} values for cast steel is available [5–7] a programme covering some of the common types was designed. This programme was based on a single type of specimen to be assessed using all three of the currently available techniques, namely linear elastic fracture mechanics, [8], crack opening displacement [9], and *J*-integral techniques [10]. All three methods were used conjointly since it is impossible to determine whether the specimen size will be adequate for the linear elastic method alone at the outset of experimentation [11].

The K_C or K_{IC} test uses a 5% change in specimen compliance, subject to certain requirements to detect fracture initiation. However, this method is not infallible and is certainly not appropriate for crack opening displacement (COD) or *J*-integral methods. In order to detect crack initiation directly the potential drop technique was used [12].

The basic specimen size chosen was 45 mm wide, W, 25 mm thick, B, and 265 mm long, notched to $a/W = 0.5$, where a is the crack length, and tested in three-point bending. This specimen was chosen on both technical and economic grounds. Six such specimens could be cut from the sound region of a keel-block casting of the available size and the overall size was felt to be the minimum representative of the cast metal containing segregation on the scale of the original cast grains.

2. Experimental methods and materials

Since the required specimen size cannot be calculated at the outset of testing, and therefore the overall cost of the programme assessed, no attempt was made to produce only K_{IC} data. Standards on K_{IC} testing are cautiously conservative and therefore costly to adhere to. Specimen size requirement for the K_{IC} test is fixed by [11]:

$$B \geqslant 2.5 \left(\frac{K_Q}{\sigma_Y}\right)^2, \qquad (1)$$

where B is the specimen thickness, σ_Y, the material yield stress and K_Q the trial value for a K_C or K_{IC}. By definition for a gross width W:

$$K_Q = \frac{P_Q Y}{BW^{1/2}} . \quad (2)$$

Here Y is a geometrical, dimensionless constant. The specimen size requirement can, therefore, be expressed by:

$$\frac{P_Q}{BW} \leqslant \frac{\sigma_Y B^{1/2}}{(2.5)^{1/2} W^{1/2} Y} . \quad (3)$$

This allows comparison with the general yield condition, i.e. the condition for yield across the ligament, which can be expressed, for this geometry as:

$$\frac{P_{GY}}{BW} = \frac{1.25\sigma_Y}{4}\left(1 - \frac{a}{W}\right)^2 . \quad (4)$$

Here P_{GY} is the load at general yield and a maximum constraint factor of 1.25 is used for this type of notch [13, 14]. In Figure 1, P_{GY}/BW is plotted against $\sigma_Y B^{1/2}$ for steels code named M, B, C, and G which are identified below. Also the equality of expression 3 is represented by the continuous line. Thus P_Q values must be below the line in Fig. 1 to meet a K_{IC} specification, and would, therefore, be around $P_{GY}/2$, the general yield levels being plotted in Fig. 1 for the basic specimen dimensions. Even though the measurement of the minimum K_{IC} toughness may not be achieved by some experiments, the resulting toughness may correspond to a K_C value for the thickness of the metal tested. It is estimated that LEFM methods are applicable for loads upto 0.8 of the general yield load [15]. Fig. 2 shows general yield loads according to Equation 4 for the four steels covered here, and average values of the P_Q measured during the fracture experiments. On this evidence the K_Q correspond to K_C values even where they do not meet the rigourous and conservative requirements of the K_{IC} test.

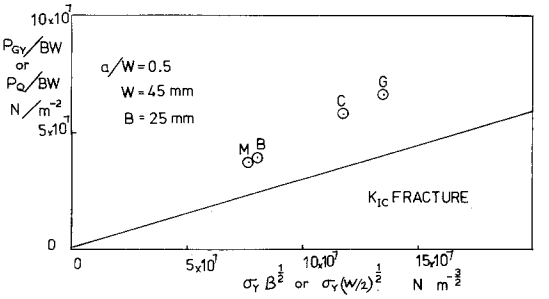

Figure 1 General yield load, P_{GY}, divided by BW and P_Q/BW for specified K_{IC} testing plotted against $\sigma_Y B^{1/2}$.

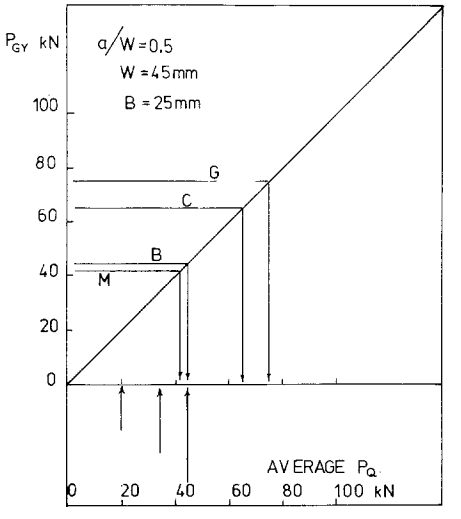

Figure 2 General yield loads, P_{GY}, versus P_Q with average measured P_Q indicated for the steels tested in the indicated specimen size.

2.1. Steels tested

The specifications, compositions and heat-treatments of the steels are shown against their code letters in Tables I, II and III, respectively.

TABLE I Specifications of steels

Code letter	B.S. specification.
B	BS 1398 E $\frac{1}{2}$Cr–$\frac{1}{2}$Mo–$\frac{1}{4}$V
C	BS 1458 A $1\frac{1}{2}$Mn–Ni–Cr–Mo
G	BS 1458 B $1\frac{1}{2}$Ni–Cr–Mo
M	BS 1956 A C–1Cr.

TABLE II Chemical compositions of the steels (wt%)

Steel	C	Si	Mn	S	P	Ni	Cr	Mo	Al	Cu	V	Sn
B	0.11	0.42	0.61	0.015	0.019	0.08	0.37	0.48	0.034	0.10	0.30	0.006
C	0.22	0.63	1.58	0.026	0.028	0.72	0.62	0.35	0.074	0.13	–	–
G	0.32	0.38	1.02	0.018	0.013	1.60	0.710	0.28	0.06	0.04	–	–
M	0.50	0.76	0.82	0.021	0.013	0.08	1.06	0.03	0.03	–	–	–

TABLE III Heat-treatment and tensile properties

Steel	Heat-treatment	Tensile strength ($MN\,m^{-2}$)	Yield or 0.2% proof stress ($MN\,m^{-2}$)
B	8 h 950° C FC; 8 h 980° C AC; 8 h 680° C FC; reheat-treated 4 h 980° C AC; 4 h 680° C FC; 8 h 700° C FC	651.4	503.6
C	4 h 680° C AC; 3 h 930° C WQ 4 h 600° C WQ.	868.6	742.3
G	4 h 900° C FC; 4 h 880° C OQ; 1 h 640° C AC	937.9	853.2
M	4 h 920° C FC; 5 h 870° C AC; $5\frac{1}{2}$ h 635° C FC.	920.0	460.0

FC, furnace cooled; AC, air cooled; WQ, water quenched.

2.2. Test methods

2.2.1. LEFM

Specimen tolerances, the test rig for three-point bending, fatigue precracking and the clip gauge design corresponded to the requirements of the B.S.I. DD3 [11]. Notch roots were sharpened by electro-spark machining before fatigue precracking since this was found to give fatigue cracks with straight fronts. Three-point bending was carried out on an Instron machine at a cross-head speed of $0.2\,mm\,min^{-1}$.

2.2.2. COD

The clip gauge as used above was directly calibrated by micrometer and the clip gauge-cross-head movement trace automatically recorded. Crack initiation was detected by the electrical potential method described below. The clip gauge COD, V_G, was converted to the crack tip COD, δ_t, using the equations [16]:

$$\delta_t = \frac{0.45(W-a)}{0.45W+0.55a+z}\left[V_G - \frac{\gamma\sigma_Y W(1-\nu^2)}{E}\right] \quad (5)$$

for

$$V_G \geqslant \frac{2\gamma\sigma_Y W(1-\nu^2)}{E}$$

or

$$\delta_t = \frac{0.45(W-a)}{0.45W+0.55a+z}\left[\frac{V_G^2 E}{4\gamma\sigma_Y W(1-\nu^2)}\right] \quad (6)$$

for

$$V_G < \frac{2\gamma\sigma_Y W(1-\nu^2)}{E}$$

Here z is the height of the clip gauge knife edges above the face of the specimen and γ is given by the following expression values of which are listed in the B.S.I. DD 19 [16]:

$$\gamma = \frac{V_0 E}{\sigma_Y W(1-\nu^2)}$$

2.2.3. J-integral

J-integral values were estimated from single load/load point displacement curves following Rice *et al.* [10], using the expression:

$$J = \frac{2}{B(W-a)}\int_0^{\delta_{crack}} P\,d\delta_{crack}. \quad (7)$$

Here δ_{crack} is the load point displacement arising from the presence of the crack. The total load point displacement is given by:

$$\delta_{total} = \delta_{crack} + \delta_{no\ crack}$$

using the superposition principle, and to obtain δ_{crack} from the measured δ_{total} the $\delta_{no\ crack}$ was obtained from beam theory for the test piece containing no crack as:

$$\delta_{no\ crack} = \frac{PS^3}{48EI}.$$

Here S is the test span of $4W$ and I the second moment of area for the uncracked beam.

Values of J were obtained by computer numerical integration of the P versus δ_{total} curve and subtraction of the P versus $\delta_{no\ crack}$ area. The δ_{total} was measured using a differential core transducer mounted as close as possible to the load application point, to exclude rig displacements, as shown in Fig. 3. Estimates of K_{IC} were obtained from J using:

$$K_{IC}^2 = \frac{J_{IC}E}{(1-\nu^2)}. \quad (8)$$

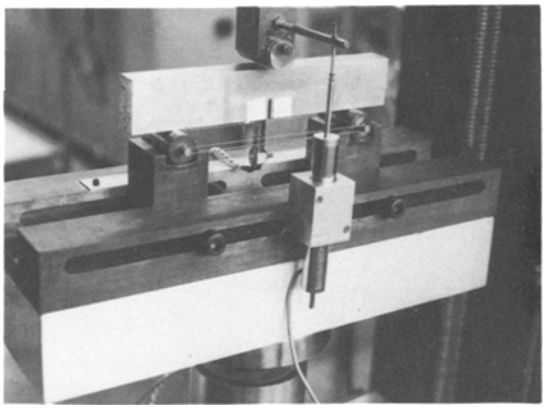

Figure 3 Test rig for three-point bend tests showing the load point displacement transducer.

The point of crack initiation was detected by the electrical potential method described below, and this measurement determined how far to integrate the load/load point displacement curve.

2.2.4. Electrical potential method

A current of 25 A was passed through the basic specimen using copper clamps for electrical connection at the far ends. The potential was picked up by spot welding 0.15 mm diameter wires, spaced at a fixed gauge length, on either side of the notch. The potential was recorded on a time base chart using a commercial recorder with its own amplifier. An accurate potential source was used to back off the signal to a suitable place on the chart. In order to attain real stability the current was passed for 1 h before measurements commenced. To gain confidence in the technique, a calibration of the potential from $a/W = 0.4$ to $a/W = 0.6$ was established using sawn notches and also using fatigue cracked notches where the change in crack length was by further fatigue cracking. The sawn notches gave an accurate calibration, fatigue cracks showed scatter on the calibration curve which arose from crack closure in the off load condition.

Actual detection of the initiation of fracture did not require the calibration since it depended on estimating the point at which the potential began to change and marking this position on the load/COD or the load/load point deflection curve.

A typical potential/time trace is shown in Fig. 4. Experiment showed that the initial small deviation did not correspond to crack extension. This deviation is, therefore, considered to arise from the COD preceding cracking. The second sharp deviation did correspond to crack extension and this point was used to curtail the load/COD and the load/load point deflection curves.

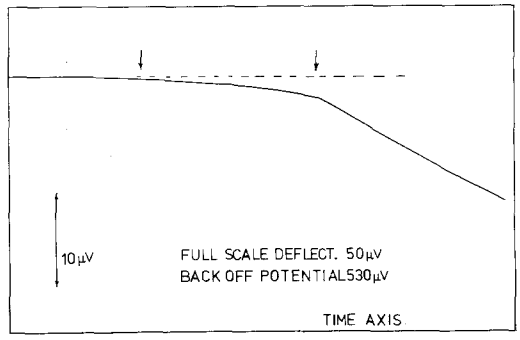

Figure 4 Typical electrical potential trace showing crack initiation.

3. Experimental results

3.1. Steel M, Ni–Cr–Mo

Fig. 5 shows the critical stress intensity factors for LEFM tests for the steel M. The K_Q values are from the 5% secant procedure. The results on the basic specimen at 25 mm thick meet the criteria for a valid K_{IC} in DD3. The ratio of the fracture load to the maximum load is close to 1.04 in all cases. The K_{IC} from tests at $B = 25$ mm is 48 ± 3 MN m$^{-3/2}$. Fig. 6 shows fracture surfaces of two of the specimens. Fatigue crack fronts are straight, the fracture is predominantly by cleavage and shear lips are negligible.

Results on variants on the standard specimen are also shown in Fig. 5. All specimens had a gross width of 45 mm but the thickness B was varied from 10 to 40 mm. Using the yield stress of 480 MN m^{-2} and the K_{IC} of 48 MN m$^{-3/2}$ all thicknesses of 25 mm or more generate valid K_{IC} values. Even down to 10 mm thickness the fracture

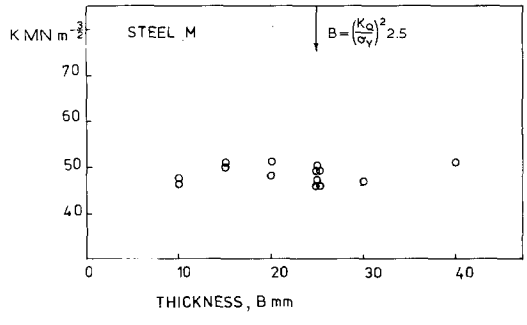

Figure 5 K_{IC} and K_C values for steel M at various thicknesses.

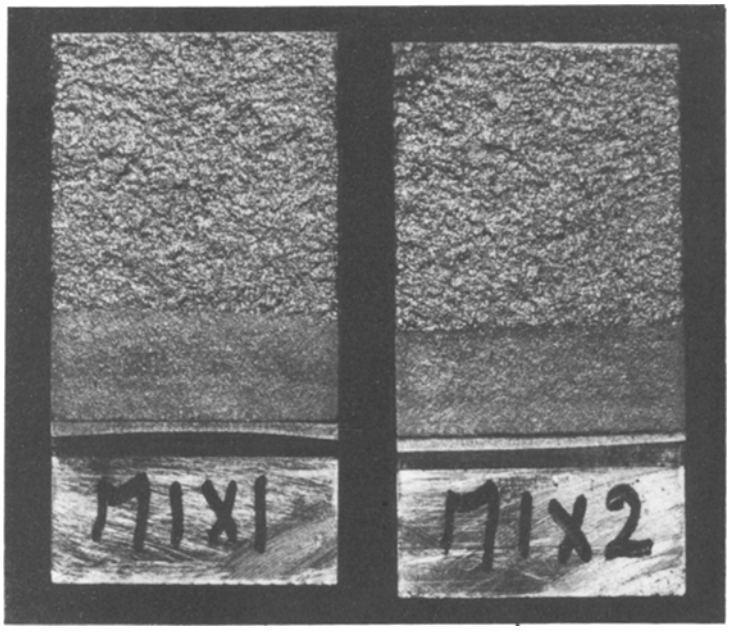

Figure 6 Fracture surfaces for 25 mm thick specimens of steel M.

toughness still corresponds to plane strain fracture as Fig. 5 shows.

The results above indicate a plane stress plastic zone size of 1.6 mm, that is almost 10% of the ligament. This being the case it is surprising that valid K_{IC} data can be obtained with such a small specimen. In fact the specimen size appears to be just sufficiently large and as will be seen below the fact that the onset of plastic behaviour is rather sudden assists these specimens to meet the linearity condition.

Results from smaller specimens, cut from the halves of those giving the above results, and with an overall length of 132 mm, are shown in Fig. 7. These results were analysed using the 5% secant method, whereas those in Fig. 8 are derived using the *J*-integral method. Surprisingly, three tests on specimens with $W = 25$ mm and $B = 35$ mm met the deviation from linearity criterion of an LEFM test [11]. However, both visual inspection and the electrical potential result showed that no crack extension had taken place at the apparent P_Q. These apparent K_C values plotted in Fig. 7 arose from a sudden onset of plastic behaviour, rather than from fracture, at around $0.8P_Q$ which gave anomalously low toughness values. In these cases the value of P_{max}/P_Q was about 1.07 in all cases. Of course it is realized that the dimensions of the specimens were far from the recommendations of the draft standard [11].

Analysis of these small specimen tests by the *J*-integral technique gave the data of Fig. 8 on which is superimposed the average K_{IC} from the larger specimens using LEMF methods. The

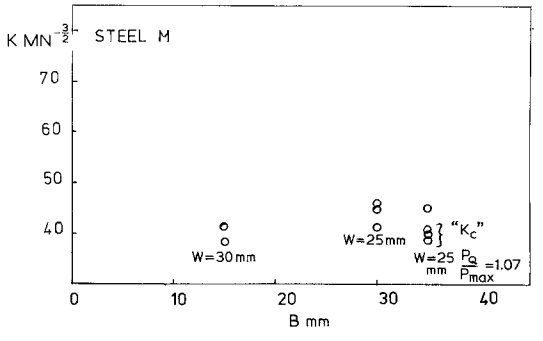

Figure 7 K_Q values corresponding to the onset of yielding in small scale specimens of steel M.

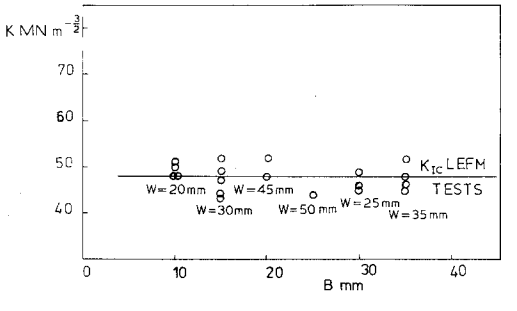

Figure 8 K_{IC} values for steel M derived from J_{IC} at fracture. Line indicates average K_{IC} from LEFM tests.

J-integral thus gave comparable results to the K_{IC} using smaller specimens and direct detection of cracking.

3.2. Steel B, Cr–Mo–V

The basic specimen size again gave valid K_{IC} according to B.S.I. DD3. These are plotted in Fig. 9 and Fig. 10 shows again mostly cleavage fracture and small shear lips. A further series of tests with varying B and with $W = 42$ mm were used for simultaneous measurements by LEFM, J-integral and COD methods. At thicknesses of 10, 15 and 20 mm these tests did not meet the thickness requirement for K_{IC}, but met the deviation from linearity test for LEFM conditions and are, therefore, K_C values for their own thickness. In fact they are most likely plane strain fracture toughnesses and the fact that they are lower than the K_{IC} at 25 mm thickness probably arises from a variation of toughness of the material.

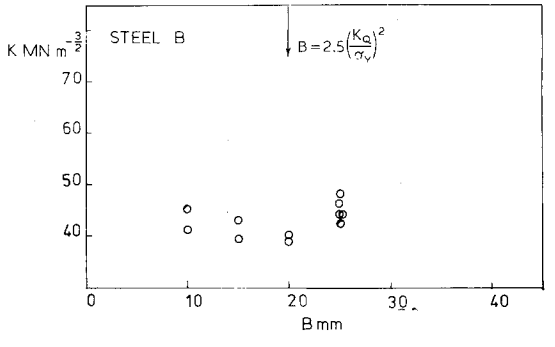

Figure 9 K_C and K_{IC} values from LEFM tests on steel B.

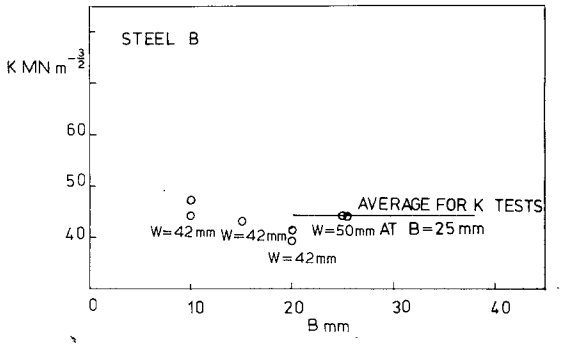

Figure 11 K_{IC} from J_{IC} for tests on steel B. Line indicates average K_{IC} from LEFM tests analysed by the secant method.

Results from the J-integral on the same specimens are shown in Fig. 11 and show comparable toughnesses to the LEFM results confirming that in this case the 5% secant method was indeed detecting crack initiation. J-integral tests on further specimens with $B = 25$ mm and $W = 50$ mm fell on the average value of the LEFM tests at $B = 25$ mm.

3.3. Steel C, Cr–Mo

Fig. 12 shows results from the steel C. The basic specimen design again gave valid K_{IC} results as did a 30 mm thick specimen. Fig. 13 shows the fracture surfaces with small but recognizable shear lips. Also shown in Fig. 12 are results for tests with varying B but $W = 45$ mm. The two low toughnesses arrowed in Fig. 12 met the LEFM linearity condition, although not the thickness condition. In fact, in these two points alone, the

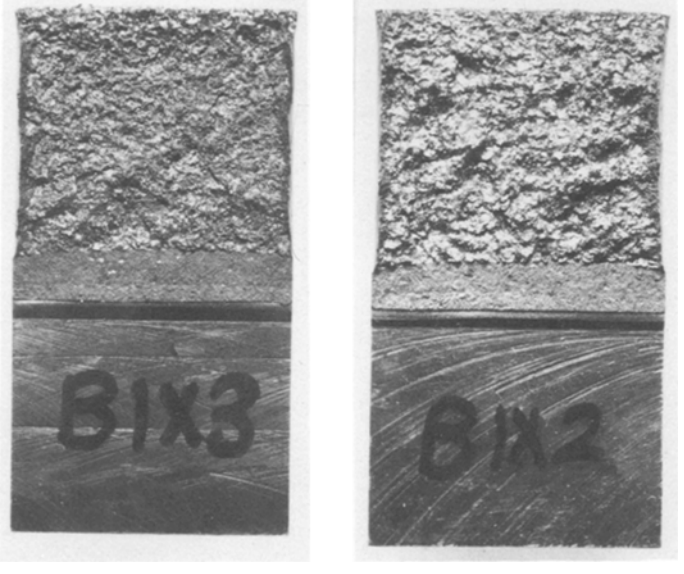

Figure 10 Fracture surfaces for 25 mm thick specimens of steel B.

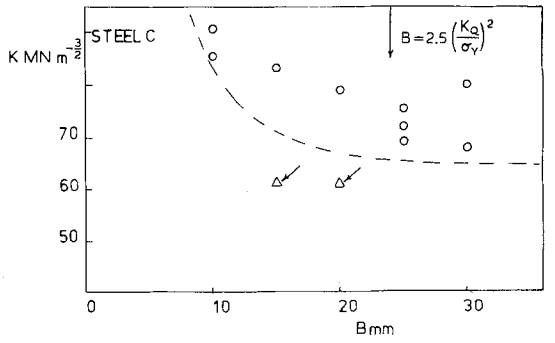

Figure 12 K_C and K_{IC} for tests on steel C derived from LEFM tests and the secant method, arrowed tests showed no crack initiation by electrical potential.

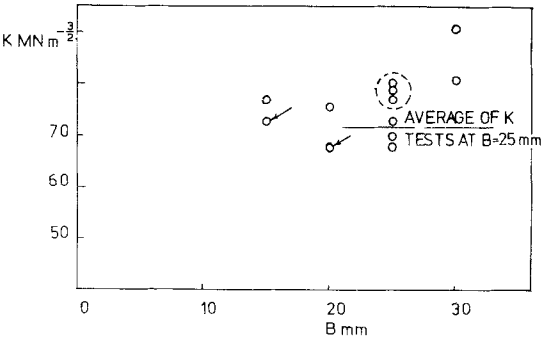

Figure 14 K_C and K_{IC} from J values for steel C. Circled tests show results derived with no subtraction of $\delta_{no\ crack}$. Arrowed tests show K values from J at fracture initiation on the same tests arrowed in Fig. 12.

P_Q did not correspond to crack initiation but to the sudden onset of plastic behaviour. Crack initiation occurred at a higher load as detected by the electrical potential method. These results would also be ruled out by DD3 since the ratio P_{max}/P_Q was about 1.7, above the limit of 1.1 set to exclude this type of plastic behaviour.

Fig. 14 shows the same tests arrowed as in Fig. 12. The K values at crack initiation derived from the J-integral method show higher toughnesses than those derived anomalously from the 5% secant method in Fig. 12. Tests at $B = 25$ mm give fracture toughnesses in agreement with the K_{IC} values of Fig. 12. The circled results indicate the overestimate of toughness which arises if the δ_{total} is used to determine J without subtracting

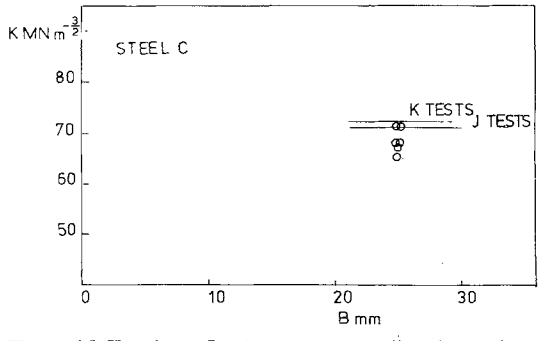

Figure 15 K_{IC} from J_{IC} for tests on small scale specimens of steel C.

$\delta_{no\ crack}$. Scatter on other values in this figure is felt to reflect variation in the material toughness.

Figure 13 Fracture surfaces for 25 mm thick specimens of steel C.

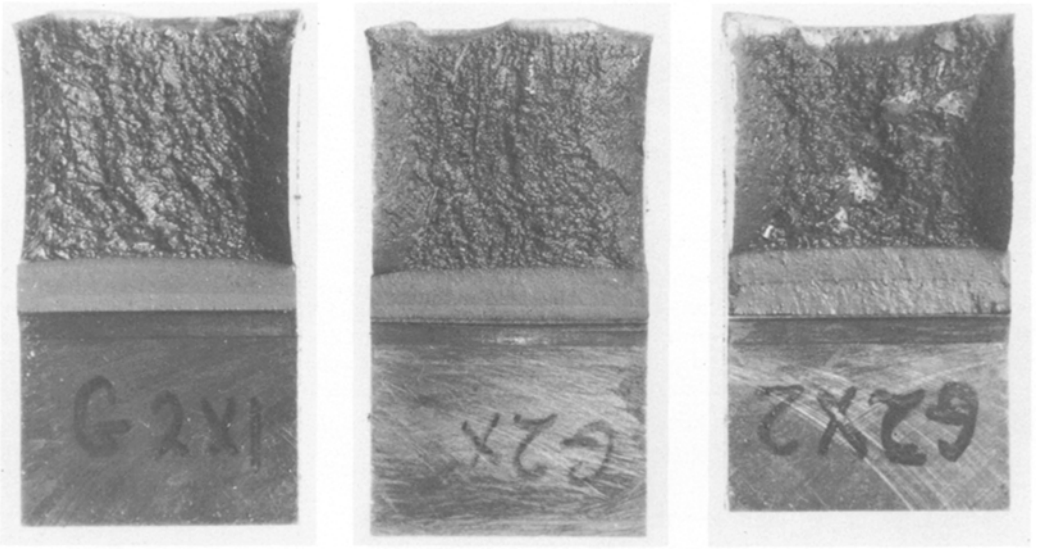

Figure 16 Fracture surfaces of 25 mm thick specimens of steel G.

Fig. 15 shows tests on specimens cut from the halves of the basic specimen type. The results of these tests with $B = 25$ mm and $W = 30$ or 35 mm are in good agreement with those derived by LEFM or J-integral methods from the larger test pieces.

3.4. Steel G, Ni–Cr–Mo

Steel G was the highest strength steel of the four and it might have been expected easier to measure its toughness. In fact it was the toughest steel as is apparent from the size of the shear lips on the basic test specimen shown in Fig. 16. Specimens taken from two different cast blocks showed a great deal of scatter in the results and also the specimen size was not generally large enough to give LEFM conditions. The tests represented in Fig. 17 met the deviation from linearity condition and are, therefore, K_C values. Results from the J-integral testing showed similar scatter.

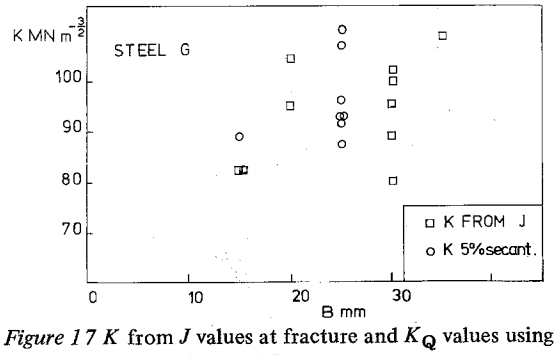

Figure 17 K from J values at fracture and K_Q values using the secant method for steel G.

3.5. Crack opening displacement tests

Crack opening displacements were small in these steels but did afford an opportunity to confirm theory with experiment where initiation was directly determined by the electrical potential method. In all cases the appropriate equation to convert clip gauge to crack tip COD was Equation 6. Having calculated this was converted to K through:

$$K = [n\delta_t\sigma_Y E/(1-\nu^2)]^{1/2}. \qquad (9)$$

Comparison of this value with K_{IC} determined by LEFM and the J-integral allowed n to be determined. Wells [14] estimated n, the stress intensification factor defined as the local elevation of the yield stress arising from constraints, as about 2.1 for plane strain conditions, and as 1.0 for plane stress tests. Intermediate values would occur in mixed fractures.

In steel M, there was no significant variation of δ_t with thickness from 15 to 35 mm. The average δ_t was 0.018 ± 0.003 mm. Also n varied from 1.0 to 1.5 with an average of 1.2 using the average K_{IC} of 48 $MNm^{-3/2}$ from LEFM tests at $B = 25$ mm.

Steel B did appear to show a variation of δ_t with thickness, average values being given below, assuming a K_{IC} of 44 MN m$^{-3/2}$ from the other tests. In view of the fact that the values of δ_t are ± 0.002 mm this seems a reasonable experimental confirmation of the estimates by Wells.

B (mm)	δ_t (mm)	n
10	0.016	1.0
15	0.014	1.3
20	0.010	1.7
25	0.010	1.7

The results from steel C also showed a small variation of δ_t with thickness with $\delta_t = 0.026$ mm at $B = 15$ mm and $\delta_t = 0.018$ mm at $B = 35$ mm. Assuming a K_{IC} of 72 MN m$^{-3/2}$ from the LEFM results this indicates a variation of n from 1.0 to 1.8.

In view of the scatter in test results on steel G, a check on the value of n is not feasible. Also the δ_t appeared to increase rather than decrease with increasing thickness from $\delta_t = 0.026$ mm at $B = 15$ mm to $\delta_t = 0.050$ mm at $B = 30$ mm. Such results probably arise from variation of the material toughness from place to place in the cast block.

4. Discussion of results

The results shown here are on steels shown to be free of defects by radiographic examination, but the results cannot be taken as representative of the *in situ* properties of similar steels in the form of castings. Variation of casting procedure, the shape and size of casting and the resulting cooling rates may well influence toughness. These are further factors to be explored. Indeed the heat-treatment given to steel B was found, by the end of this testing programme, to be obsolete as far as industrial practice is concerned, modified heat-treatments giving greater toughnesses [17]. Nevertheless these initial assessments are felt to be helpful in that they help decide the scale of testing for future programmes to discover accurately the defect tolerances of these steels.

In all but steel G the basic specimen size gave valid assessments of the K_{IC}. Clearly in steel G the effects of position of the test piece in the casting and the effects of micro and macro-segregation need to be carefully assessed; however, the tests here do show the great, relative, toughness of this type of steel, and allow a better guess at the size of test piece necessary to make accurate toughness measurements.

An important feature in steels M and C is that yield at the crack tip is delayed upto a reasonably high load and then spreads rapidly. This gives rise to a load/COD curve which can be apparently linear elastic, plus a deviation arising from a compliance change due to cracking, when in fact no cracking has taken place. The LEFM methods of DD3 should be adequate to exclude this type of behaviour with much larger specimens than those tested here where it is necessary to confirm, by direct detection, that cracking has occurred.

In steels M and B the toughness did not rise above the K_{IC} level down to thicknesses of 10 mm. The K_{IC} is, therefore, the appropriate design property for all practical castings. In the case of steel C some increase in toughness with smaller thicknesses was observed; however, practical design would still be on the basis of K_{IC}.

The J-integral technique was a practical and accurate method of toughness assessment even with specimens as small as 20 mm wide and 10 mm thick, for instance, in the case of steel M. Naturally, a direct crack detection method was required, and also slightly more sophisticated computation. In detail the load/load point deflection curve was expressed accurately by a polynomial expression which was integrated numerically by computer.

Crack opening displacement methods are more accurate with higher toughness materials than those tested here. Typically the crack tip displacements at fracture initiation were around 0.020 ± 0.003 mm. This means a maximum error of around 30% in the property measured, arising mostly from the small, absolute size of the displacements. In spite of this, the results confirm the stress intensification factor, that is the degree of elevation of the yield stress, by constraints, in the plastic zone, to be between 1.0 and 2.0. The only case in which a small variation in δ_t with thickness appeared to be significant showed this kind of variation, although the LEFM tests did not show a corresponding fall in K_C to K_{IC} over the same thickness range.

5. Conclusions

The minimum specimen size for K_{IC} measurement in steels M, B, and C is about 45 mm wide using LEFM [8, 11] techniques, although because the onset of yielding is sudden in these steels, a speci-

men of twice this size would be recommended where direct detection of crack initiation is not made. *J*-integral techniques give toughness values comparable in accuracy with LEFM methods, even on smaller specimens, but here direct detection of the crack initiation is essential. COD methods are not really appropriate for the steels surveyed here, mainly because they do not have large and, therefore, accurately measurable values of COD at fracture. Nevertheless, the results confirm qualitatively the estimates of Wells of the operative stress intensification.

Acknowledgements

The authors would like to thank the staff at S.C.R.A.T.A. for the provision of test materials, for encouragement and helpful discussions, and for the financial support of one of us during the final year of this project.

References

1. P. RICE, *Acier-Steel-Stahl* **40** (1975) 297.
2. A.S.M.E. Code of Practice for the Construction of Pressure Vessels.
3. A.S.T.M. Standard E71-64.
4. J. D. LAVENDER, Proceedings of the Conference on Quality Control and the Significance of Mech. Props., S.C.R.A.T.A. (1975).
5. H. D. GREENBERG and D. CLARK, *Mat. Eng. Quart.* 9 (1969) 30.
6. J. BRADSHAW and W. J. JACKSON, *J. Res. S.C.R.A.T.A.* 8 (1970) 2.
7. F. KUZUCU, Thesis, University of Birmingham (1972).
8. J. E. SRAWLEY, "Practical Fracture Mechanics for Structural Steel" edited by M. O. Dobson (U.K.A.E.A., 1969).
9. A. A. WELLS, Proceedings of Crack Propagation Symposium, Cranfield, 1961 Vol. 1 (College of Aeronautics, Cranfield, 1962).
10. J. R. RICE, P. C. PARIS and J. G. MERKLE, ASTM, STP 536.
11. B.S.I., Methods for Plane Strain Fracture Toughness (K_{IC}) Testing, DD3 (1972).
12. D. M. GILBEY and S. PEARSON, Royal Aircraft Est. Tech. Rpt. No. 66402.
13. A. P. GREEN and B. B. HUNDY, *J. Mechs Phys. Solids* 4 (1956) 128.
14. A. A. WELLS, Int. Rpt. Dept. Civ. Eng., Queens University, Belfast (1970).
15. J. E. SRAWLEY and W. F. BROWN, ASTM, STP 381 (1965) p. 153.
16. B.S.I. Methods for Crack Opening Displacement (COD) Testing, DD19 (1972).
17. M. KIRKE, personal communication.

Received 7 April and accepted 4 May 1976.